

Copyright is owned by the Author of the thesis. Permission is given for a copy to be downloaded by an individual for the purpose of research and private study only. The thesis may not be reproduced elsewhere without the permission of the Author.

A MINERALOGICAL AND TEXTURAL STUDY
OF
THE CENTRAL NORTH ISLAND TEPHRA, OKAREKA ASH
AND
ITS OVERLYING TEPHRIC LOESS DEPOSITS

A Thesis Presented as Partial Fulfillment for
the Degree of Master of Science in Soil Science

by

Lynette Anne Benny

Massey University,
New Zealand

1982

ACKNOWLEDGEMENTS

I wish to thank my supervisors Dr. J.H. Kirkman, and Mr. R.B. Stewart for their guidance, encouragement and advice during my thesis work.

I wish also to extend my thanks to Dr. W.A. Pullar and Mr N.M. Kennedy, Soil Bureau, Rotorua, for their invaluable assistance in collecting soil samples for this study, and worthwhile discussion in the field.

I am grateful to Mr. D. Hopcroft and Mr. R.J. Bennett of the Electron Microscope Lab. D.S.I.R., for their technical assistance in the electron optical work, and printing of the electron micrographs.

To Miss. J.S. Rowarth and Mr. R.C. Wallace, my thanks for your critical reading of, and helpful comments about the manuscript.

I would also like to thank my mother, Mrs. A.F. Benny, who typed this thesis, and finally, both my parents for their continuing support.

ABSTRACT

In Central North Island, New Zealand, Post-Okareka tephric loess rests upon Okareka Ash (c.17,000 years B.P.). Tephric loess accumulation occurred under semi-arid conditions which coincided with glacial advances in southern areas of New Zealand.

Morphological and grain-size evidence indicates the tephric loess has been derived from a localised source, most probably that of Okareka Ash material, reworked and redeposited by aeolian processes. Optical and electron optical evidence reveals that Okareka Ash particles are angular and relatively unweathered, whereas tephric loess grains are subangular and more weathered.

The sand and clay mineralogy of the tephra and tephric loess are similar. Sand fractions contain mainly rhyolitic volcanic glass, quartz, plagioclase feldspar, biotite, hypersthene, hornblende, titanomagnetite and traces of cristobalite, tridymite and augite, whereas clay fractions contain halloysite, allophane, imogolite and gibbsite in varying amounts.

Grain-size analysis reveals Okareka Ash deposits show decreasing mean grain-size with increasing distance from source, are poorly-sorted, fine-skewed, and leptoplatic. In contrast to tephra, tephric loess samples exhibit a narrow mean grain-size range, and are better sorted, but show similar skewness and kurtosis values to ash. Grain-size results also indicate that due to minimal weathering of Okareka Ash and Post-Okareka loess, the distinction between the two deposits is less well-defined than data from similar deposits reported by Fisher (1966). Furthermore, where ash deposits are thin, in distal areas from source, and under certain environmental conditions, textural and morphological characteristics of the tephra are similar to those of the tephric loess. Nevertheless, grain-size parameters may be used to differentiate airfall tephra and tephric loess deposits, although this

differentiation is enhanced by post-depositional weathering.

The contrasting clay mineralogies of tephra and tephric loess samples from sections of similar topography, altitude, drainage and rainfall, illustrates the problems of field sampling in weathering studies.

TABLE OF CONTENTS

	<u>Page No.</u>
Acknowledgements	ii
Abstract	iii
Table of Contents	v
List of Tables	viii
List of Figures	ix
Nomenclature	xiii
Abbreviations	xiv
 Chapter 1: Introduction	 1
SECTION A: <u>Mineralogy and Morphology</u>	
 Chapter 2: Literature Review	 3
2.1 Distribution of airfall deposits in New Zealand	3
2.2 Tephra and loess deposits of Central North Island	6
2.3 Okareka Ash and overlying loess deposits	10
2.4 Weathering studies of tephra and tephra-derived soils	12
 Chapter 3: Materials and Methods	 19
3.1 Field Techniques	19
3.2 Instrumental Techniques	23
 Chapter 4: Results	 26
4.1 Sand and silt mineralogy	26
4.1.1 Okareka Ash Formation: Trunk Rd	26
4.1.2 Okareka Ash: remaining sections	26
4.1.3 Post-Okareka loess	28
4.2 Sand and silt morphology	29
4.2.1 Okareka Ash	29
4.2.2 Post-Okareka loess	35
4.3 Clay mineralogy	46
4.3.1 Okareka Ash: Trunk Rd	46
4.3.2 Okareka Ash: remaining sections	49

	<u>Page No.</u>
4.3.3 Post-Okareka loess: Trunk Rd	59
4.3.4 Post-Okareka loess: Gavin Rd and Te Ngae sections	59
4.3.5 Post-Okareka loess: remaining sections	61
4.3.6 Gibbsite in clay fractions of ash and loess deposits	71
 Chapter 5: Discussion	 77
5.1 Okareka Ash sand and silt mineralogy	77
5.2 Post-Okareka loess sand and silt mineralogy	78
5.3 Okareka Ash sand and silt morphology	80
5.4 Post-Okareka loess sand and silt morphology	81
5.5 Weathering in Okareka Ash and Post- Okareka loess deposits	82
 SECTION B: <u>Grain-size Analysis</u>	
 Chapter 6: Literature Review	 91
6.1 Textural Studies	91
 Chapter 7: Materials and Methods	 95
7.1 Analytical Techniques	95
 Chapter 8: Results and Discussion	 96
8.1 Grain-size parameters	96
8.1.1 Mean grain-size: Okareka Ash	96
8.1.1 Mean grain-size: Post-Okareka loess	98
8.1.2 Sorting	103
8.1.3 Skewness	105
8.1.4 Kurtosis	106
8.1.5 Mean grain-size versus sorting	109
8.1.6 Mean grain-size versus skewness, and kurtosis	111
8.1.7 Mean grain-size versus $M_z / M_z + \sigma_I$	111
8.1.8 Mean grain-size versus $K_G / K_G + M_z$	115

	<u>Page No.</u>
Chapter 9: Conclusions	118
References	121
Appendices	131

LIST OF TABLES

<u>Table No.</u>		<u>Page No.</u>
1	Correlation of late Pleistocene tephra deposits in Central North Island, with North Westland glacial advances	7
2	Frequency of mineral species (percent) in very fine sand (63 - 125 μ m) and fine sand (125 - 250 μ m) fractions from selected beds in Okareka Ash Formation, Trunk Rd section	27
3	Summary of Mineralogical and Morphological Results	76

LIST OF FIGURES

<u>Figure No.</u>		<u>Page No.</u>
1	Generalised map of airfall deposits in North Island, New Zealand	5
2	Isopachs showing distribution of Okareka Ash	11
3	Site locations, Rotorua district, Central North Island	20
4	Stratigraphy of transect sections	21
5	Stratigraphy of Te Ngae, Trunk Rd and Gavin Rd sections	22
6	Scanning electron micrographs of: A - rhyolitic volcanic glass particles, B - plagioclase feldspar grain exhibiting albite (multiple) twinning, separated from Okareka Ash samples	30
7	Scanning electron micrographs of: A - quartz grains, B - bipyramidal-shaped quartz grain, separated from Okareka Ash samples	31
8	Scanning electron micrographs of hypersthene grains separated from: A - Okareka Ash samples, B - Post-Okareka loess samples	32
9	Scanning electron micrographs of hornblende grains separated from: A - Okareka Ash samples, B - Post-Okareka loess samples	33
10	Scanning electron micrographs of biotite mica grains separated from: A - Okareka Ash samples, B - Post-Okareka loess samples	34
11	Scanning electron micrographs of titanomagnetite grains separated from: A - Okareka Ash samples, B - Post-Okareka loess samples	36
12	Scanning electron micrographs of Okareka Ash particles separated from sections: A - close to source (R_{AL}), B - intermediate (C_A), and C - furthestest (E_A) to ash source	37
13	Scanning electron micrograph of plagioclase feldspar grains separated from Post-Okareka loess samples	38

<u>Figure No.</u>		<u>Page No.</u>
14	Scanning electron micrographs of plagioclase feldspar grains separated from Post-Okareka loess samples: A - feldspar prism coated with short-range order material, and at B - higher magnification, C - feldspar prism showing dissolution etch marks, and D - at higher magnification	39 40
15	Scanning electron micrographs of: A - exposed cleavage planes in a biotite mica grain, and B - a pumiceous particle separated from Post-Okareka loess samples	42
16	Scanning electron micrographs of: A - a silt-sized aggregate, with, B - clay-size material forming on grain fragments within the aggregate, which has been separated from Post-Okareka loess samples	43
17	Scanning electron micrographs of Post-Okareka loess particles separated from sections: A - close (AL_1), B - intermediate (CL_2), and C - furthest (EL_1) to ash source	45
18	X-ray diffraction patterns (\bar{A}) of the clay ($<1.0\mu m$) fraction from Okareka Ash, Ngongotaha section	47
19	Infra-red spectra (cm^{-1}) of Okareka Ash clay ($<1.0\mu m$) fractions from selected sections	48
20	Transmission electron micrograph of $<1.0\mu m$ size clay of Okareka Ash at Trunk Rd section (R_A bed)	50
21	Transmission electron micrograph of $<1.0\mu m$ size clay of Okareka Ash at Trunk Rd section (R_{AL} bed)	51
22	Transmission electron micrograph of $<1.0\mu m$ size clay of Okareka Ash at Trunk Rd section, showing surface boiling affects on halloysite tubes and hexagonal-shaped material	52
23	Differential thermal curves ($^{\circ}C$) of Okareka Ash clay ($<1.0\mu m$) fractions from	53

<u>Figure No.</u>	<u>Page No.</u>
	selected sections
24	Transmission electron micrograph of <math><1.0\mu\text{m}</math> size clay of Okareka Ash at Te Ngae section 55
25	Transmission electron micrograph of <math><1.0\mu\text{m}</math> size clay of Okareka Ash at Pukehangi Rd section 56
26	Transmission electron micrographs of <math><1.0\mu\text{m}</math> size clay of Okareka Ash at: A - Tarukenga and B - Highland Hill sections 58
27	Transmission electron micrograph of <math><1.0\mu\text{m}</math> size clay of Post-Okareka loess at Trunk Rd section 60
28	Infra-red spectra (cm^{-1}) of Post-Okareka loess clay (<math><1.0\mu\text{m}</math>) fractions from selected sections 63
29	Differential thermal curves ($^{\circ}\text{C}$) of Post-Okareka loess clay (<math><1.0\mu\text{m}</math>) fractions from selected sections 64
30	Transmission electron micrograph of <math><1.0\mu\text{m}</math> size clay of Post-Okareka loess at Pukehangi Rd section 66
31	Transmission electron micrograph of <math><1.0\mu\text{m}</math> size clay of Post-Okareka loess at Ngongotaha section 68
32	Transmission electron micrograph of <math><1.0\mu\text{m}</math> size clay of Post-Okareka loess at Tarukenga section 69
33	Transmission electron micrograph of <math><1.0\mu\text{m}</math> size clay of Post-Okareka loess at Dalbeth Rd section 70
34	Transmission electron micrograph of <math><1.0\mu\text{m}</math> size clay of Post-Okareka loess at Highland Hill section 72
35	Differential thermal curves ($^{\circ}\text{C}$) of Post-Okareka loess (basal sample) silt and clay fractions at Dalbeth Rd section 73
36	Differential thermal curve ($^{\circ}\text{C}$) of a crushed sample of well-ordered crystalline gibbsite 74

<u>Figure No.</u>	<u>Page No.</u>
37	97
Mean grain-size of Okareka Ash and Post-Okareka loess deposits in relation to distance from ash source	
38	99
Grain-size cumulative curves for Okareka Ash deposits	
39	100
Variation in sand, silt and clay percent in Okareka Ash and Post-Okareka loess deposits in relation to distance from ash source	
40	101
Grain-size cumulative curves for Post-Okareka loess deposits	
41	102
Grain-size cumulative curves of Okareka Ash and Post-Okareka loess deposits from Ngongotaha section	
42	104
Sorting of Okareka Ash and Post-Okareka loess deposits in relation to distance from ash source	
43	107
Skewness of Okareka Ash and Post-Okareka loess deposits in relation to distance from ash source	
44	108
Kurtosis of Okareka Ash and Post-Okareka loess deposits in relation to distance from ash source	
45	110
Mean grain-size versus sorting plots for Okareka Ash and Post-Okareka loess deposits	
46	112
Mean grain-size versus skewness plots for Okareka Ash and Post-Okareka loess deposits	
47	113
Mean grain-size versus kurtosis plots for Okareka Ash and Post-Okareka loess deposits	
48	114
Variation of mean grain-size versus the mean grain-size - sorting coefficient ratio ($M_z/M_z + \sigma I$) for Okareka Ash and Post-Okareka loess deposits	
49	116
Variation of mean grain-size versus the kurtosis - mean grain-size coefficient ratio ($K_G/K_G + M_z$) for Okareka Ash and Post-Okareka loess deposits	

NOMENCLATURE

Sections: (except for Trunk Rd, sections sampled are given a letter symbol, listed below, with increasing distance from Okareka Ash source)

- G Gavin Rd
- A Okareka Quarry
- I Lynmore
- H Te Ngae
- B Pukehangi Rd
- J Ngongotaha
- C Tarukenga
- D Dalbeth Rd
- E Highland Hill
- K Kuhatahi

At Trunk Rd section, due to the thickness of Okareka Ash, samples were labelled according to -

firstly, the predominance of

R rhyolitic (pale grey)

or B basaltic (dark grey-black) material

and secondly, the grain-size by a letter subscript -

A ash

L lapilli

c coarse

f fine

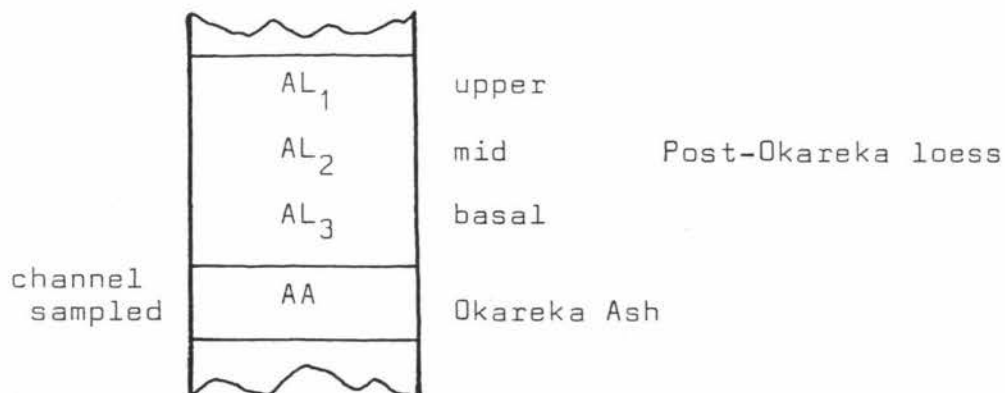
Ash and Loess: loess samples were labelled -

L loess

A Ash

and given a number subscript, from top to base, depending upon the number of samples taken -

e.g. Okareka Quarry - section A



ABBREVIATIONS

Al	Aluminium
Å	angstrom (10^{-7} m)
An	anorthite
Cpx	augite
Bt	biotite mica
cm	centimetre (10^{-2} m)
°C	degrees celsius
DTA	differential thermal analysis
Fds	feldspar (includes alkali and plagioclase)
g	gram
>	greater than
Hb	hornblende
H	hydrogen
Opx	hypersthene
IR	infra-red spectroscopy
kHz	kilohertz
km	kilometre
Kw	kilowatt
K_G	kurtosis
<	less than
Mz	mean grain-size
m	metre
µm	micrometre (10^{-6} m)
mg	milligram (10^{-3} g)
mm	millimetre (10^{-3} m)
O	oxygen
%	percent
Qz	quartz
∅	phi scale
(v)ps	(very) poorly-sorted
RI	refractive index
SEM	scanning electron microscope
Si	silica
SK_I	skewness
(s)fs	(strongly) fine-skewed
sym	symmetrical
∅I	sorting
θ	theta

FeO titanomagnetite
TEM transmission electron microscope
VG volcanic glass (rhyolitic)
XRD X-ray diffraction

N.B. for consistency all grain-size calculations were carried out at μm sizes to equal ϕ (phi-scale) divisions (e.g. $63\mu\text{m} = 4.5\phi$)